Plant Molecular Biology (2024) 114:60
https://doi.org/10.1007/s11103-023-01401-0

Pyruvate kinase 2 from *Synechocystis* sp. PCC 6803 increased substrate affinity via glucose-6-phosphate and ribose-5-phosphate for phosphoenolpyruvate consumption

Masahiro Karikomi[1] · Noriaki Katayama[1] · Takashi Osanai[1]

Received: 8 June 2023 / Accepted: 30 November 2023 / Published online: 17 May 2024

Abstract

Pyruvate kinase (Pyk, EC 2.7.1.40) is a glycolytic enzyme that generates pyruvate and adenosine triphosphate (ATP) from phosphoenolpyruvate (PEP) and adenosine diphosphate (ADP), respectively. Pyk couples pyruvate and tricarboxylic acid metabolisms. *Synechocystis* sp. PCC 6803 possesses two pyk genes (encoded *pyk1*, sll0587 and *pyk2*, sll1275). A previous study suggested that *pyk2* and not *pyk1* is essential for cell viability; however, its biochemical analysis is yet to be performed. Herein, we biochemically analyzed *Synechocystis* Pyk2 (hereafter, *Sy*Pyk2). The optimum pH and temperature of *Sy*Pyk2 were 7.0 and 55 °C, respectively, and the K_m values for PEP and ADP under optimal conditions were 1.5 and 0.053 mM, respectively. *Sy*Pyk2 is activated in the presence of glucose-6-phosphate (G6P) and ribose-5-phosphate (R5P); however, it remains unaltered in the presence of adenosine monophosphate (AMP) or fructose-1,6-bisphosphate. These results indicate that *Sy*Pyk2 is classified as PykA type rather than PykF, stimulated by sugar monophosphates, such as G6P and R5P, but not by AMP. *Sy*Pyk2, considering substrate affinity and effectors, can play pivotal roles in sugar catabolism under nonphotosynthetic conditions.

Key message

Glucose-6-phosphate and ribose-5-phosphate increased *Synechocystis* Pyk2 affinity for PEP, possibly contributing to PEP consumption under nonphotosynthetic conditions.

Keywords Glycolysis · Microalgae · Pyruvate kinase · *Synechocystis* sp. PCC 6803

Introduction

Cyanobacteria can utilize CO_2 via photosynthesis to synthesize value-added metabolites for a low-carbon society (Hidese et al. 2020; Angermayr et al. 2014; Hasunuma et al. 2018). *Synechocystis* sp. PCC 6803 (hereafter, *Synechocystis*) is a unicellular, non-nitrogen fixing model cyanobacterium that is utilized for bioproduction (Ruffing 2011; Wang et al. 2012; Yu et al. 2013). *Synechocystis* produces carboxylic acids, such as D-lactate, and polyhydroxy-3-butyrate (PHB), as food additives and bioplastics; these two metabolites are derived from pyruvate (Osanai et al. 2015; Hidese et al. 2020; Ito et al. 2017; Carpine et al. 2017).

Various groups have widely studied primary carbon metabolism in *Synechocystis*, including metabolic regulation, pathway identification, and metabolic enzyme biochemistry (Fig. 1). *Synechocystis* has several glucose catabolic routes, such as the Embden–Meyerhof–Parnas (EMP) and oxidative pentose phosphate (OPP) pathways (You et al. 2014). *Synechocystis* has a unique tricarboxylic acid (TCA) cycle lacking 2-oxoglutarate dehydrogenase and possessing alternative pathways, such as a γ-butyric amino acid (GABA) shunt (Zhang and Bryant 2011; Xiong et al. 2014). The properties of the enzymes of the *Synechocystis* TCA cycle have been studied, including those of citrate synthase (CS encoded by *gltA*, sll0401) (Ito et al. 2019), aconitase (Aco encoded by *acnB*, slr0665) (Nishii et al. 2021; de Alvarenga et al. 2020), isocitrate dehydrogenase (IDH encoded

✉ Takashi Osanai
tosanai@meiji.ac.jp

[1] School of Agriculture, Meiji University, 1-1-1, Higashimita, Tama-Ku, Kawasaki, Kanagawa 214-8571, Japan

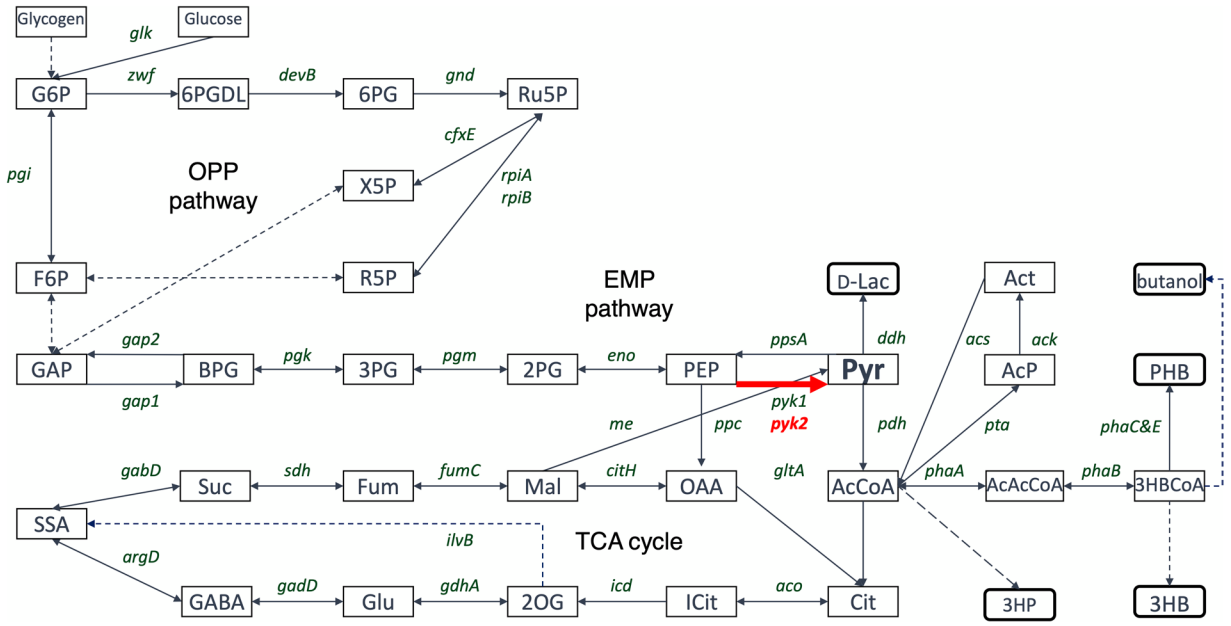

Fig. 1 Pathway map of *Synechocystis* sp. PCC 6803 (*Synechocystis*). The metabolic maps of the Embden–Meyerhof–Parnas (EMP) pathway/gluconeogenesis, oxidative pentose phosphate (OPP) pathway, pyruvate metabolism, and tricarboxylic acid (TCA) cycle. The gene names encoding metabolic enzymes in *Synechocystis* were obtained from the Kyoto Encyclopedia of Genes and Genomes database. The rounded rectangle indicated value-added metabolites from *Synechocystis*

by *icd*, slr1289) (Muro-Pastor and Florencio 1992), malate dehydrogenase (MDH encoded by *citH*, sll0891) (Takeya et al. 2018), malic enzyme (ME encoded by *me*, sll0721) (Katayama et al. 2022), and succinate dehydrogenase (SDH encoded by *sdh*, sll0823 and sll1625) (Cooley and Vermaas 2001). Two enzymes, phosphoenolpyruvate carboxylase (PEPC) and pyruvate kinase (Pyk), catalyze specific reactions that provide carbon sources to the TCA cycle. *Synechocystis* possesses one PEPC encoded by *ppc* (sll0920) and two Pyks encoded by *pyk1* (sll0587) and *pyk2* (sll1275) (Kaneko et al. 1996). *Synechocystis* PEPC exhibits a unique allosteric regulation uninhibited by several metabolic effectors, such as malate, aspartate, and fumarate (Takeya et al. 2017; Scholl et al. 2020). Pyk enzymatic activity from *Synechocystis* cell cultures has been measured and reported to be higher under nonphotosynthetic conditions than those under photoautotrophic and mixotrophic conditions (Knowles and Plaxton 2003).

The phylogenetic analysis of the Pyks of *Synechocystis* revealed bacterial Pyk and an evolutionary distance between the two isoforms of Pyks, Pyk1 (hereafter, *Sy*Pyk1) and Pyk2, in cyanobacteria (Haghighi 2021). Bacterial Pyk is classified as PykA and PykF, and sugar monophosphates, such as AMP, G6P, and R5P, stimulate PykA. PykF is activated by sugar diphosphates, such as FBP, in *Escherichia coli* (Kornberg and Malcovati 1973; Waygood et al. 1975, 1976). *Sy*Pyk2 is classified into *pykF*, and *pyk2* knockout causes severe growth defects (Yao et al. 2020). In a previous study, the biochemical analysis of the Pyk of another cyanobacterium, *Synechococcus* sp. PCC 6301 (hereafter, *Synechococcus* Pyk), was reported to be homologous to that of *Synechocystis pyk2*, suggesting that ATP and TCA metabolism inhibited *Synechococcus* Pyk, thus indicating its roles under dark conditions (Knowles et al. 2001). *pyk2* expression increases in the wild-type strain in the presence of glucose (Kaniya et al. 2013). *pyk2* expression patterns remain unchanged during the day/night cycle (Saha et al. 2016). These reports indicate that *Sy*Pyk2 is essential during photosynthetic and nonphotoautotrophic conditions in *Synechocystis*. This study revealed the regulatory properties of *Sy*Pyk2 via biochemical analysis and demonstrated that sugar phosphates activated *Sy*Pyk2 activity.

Materials and methods

Construction of cloning vector for recombinant *Sy*Pyk2

The amino acid sequence of Pyk2 (sll1275) polypeptide was obtained from the Kyoto Encyclopedia of Genes and Genomes database (https://www.genome.jp/kegg/) and synthesized by Eurofins Genomics Japan (Tokyo, Japan). The synthesized fragment was inserted within the BamHI–XhoI site of the vector pGEX6P-1 (GE Healthcare Japan, Tokyo, Japan). The cloned expression vector was transformed into

competent *E. coli* BL21 cells (Takara Bio, Shiga, Japan) and cultured in 6 mL of Luria–Bertani medium at 30 °C with shaking at 150 rpm. Recombinant *E. coli* BL21 cells from 1.2-L culture were suspended in 40 mL of phosphate-buffered saline/Tween (PBST) (1.37 M NaCl, 27 mM KCl, 81 mM Na_2HPO_4•$12H_2O$, 14.7 mM KH_2PO_4, and 0.05% Tween 20) and sonicated (model VC-750; EYELA, Tokyo, Japan). This procedure was repeated 10 times at 20% intensity for 20 s. The lysed cells were centrifuged twice at 12,500 rpm for 15 min at 4 °C. The supernatant was transferred into a 50 mL tube, and 2 mL of Glutathione Sepharose 4 B resin (Cytiva Japan, Tokyo, Japan) was added. The tubes were shaken gently for 60 min on ice. The mixture was centrifuged at 8,000 rpm for 2 min at 4 °C to remove the supernatant. The resin was transferred to a 15 mL tube and washed using PBST. After washing, the recombinant protein was eluted five times using 650 µL of glutathione-S-transferase (GST) elution buffer (50 mM Tris–HCl, pH 9.6-, and 10-mM reduced glutathione) and incubated in Vivaspin 500 MWCO 50,000 device (Sartorius, Göttingen, Germany) for protein concentration. The protein concentrations were determined using Pierce BCA Protein Assay Kit (Thermo Fisher Scientific, Rockford, IL, USA). The solution was transferred to a 1.5 mL tube, and 40 units of PreScission Protease (equivalent to the purified recombinant protein) (Cytiva) were added and allowed to stand at 4 °C for 16 h to remove GST-tag from the recombinant proteins. Approximately 750 µL of Glutathione Sepharose 4B resin was added, rotated for 1 h at room temperature to remove the cleaved tag from the solution, at 11,000 rpm for 4 min at 4 °C, and the supernatant was collected. Sodium dodecyl sulfate–polyacrylamide gel electrophoresis was performed to confirm protein purification, and gels were stained using Quick Blue reagent (Bio-Dynamics Inc. Tokyo, Japan).

Enzyme assay

All solutions were prepared using Milli-Q water; the *Sy*Pyk2 reaction was coupled with lactate dehydrogenase (LDH) from a pig heart (Wako Chemicals, Osaka, Japan) reaction and measured at 30 °C or 55 °C by monitoring NADH oxidation at 340 nm in a final volume of 1 mL. The experiments were performed using 1.88 pmol of the recombinant *Sy*Pyk2 proteins. We measured *Sy*Pyk2 activity at an intracellular condition of 30 °C and pH 7.8 (Inoue et al. 2001; Nakamura et al. 2021). Unless otherwise indicated, the assay conditions for *Sy*Pyk2 were 100 mM Tris–HCl (pH 7.8) or 100 mM MES-NaOH (pH 7.0), 15 mM $MgCl_2$ or 5 mM $MnCl_2$, 100 mM KCl, 0.2 mM NADH, 2 mM ADP-2Na, 15 units/mL desalted LDH from pig heart, and 5 mM PEP-Na. All measurements were performed using 15 mM Mg^{2+} except where indicated. One unit of *Sy*Pyk2 activity was defined as the oxidation of 1 µmol NADH per minute produced. Each effector was added 0.1 mM each: glucose-6-phosphate-2Na (G6P); fructose-6-phosphate-2Na (F6P); fructose-1, 6-bisphosphate-3Na (FBP); ribose-5-phosphate-2Na (R5P); 6-phospho-D-gluconate (6PG); adenosine monophosphate-Na (AMP); adenosine diphosphate-2Na (ADP); adenosine triphosphate-2Na (ATP); citrate-3Na; 2-oxoglutarete (2OG); succinate-2Na; fumarate; malate-Na. The results were plotted as a graph of the reaction rate to substrate and coenzyme concentration. K_m and V_{max} values were calculated by curve fitting using Kaleida Graph ver. 4.5 software and k_{cat} were calculated from the V_{max}.

Statistical analyses

Paired two-tailed Student's *t*-tests were performed to calculate the *P*-values using Microsoft Excel for Windows (Redmond, WA, USA). All experiments were conducted independently in triplicate.

Results

Purification of *Sy*Pyk2 and determination of optimal temperature and pH

We expressed GST-tagged *Sy*Pyk2 proteins in *E. coli* BL21 and purified them using affinity chromatography (Fig. 2a). *Sy*Pyk2 activity for PEP was the highest in MES-NaOH buffer at pH 7.0 and temperature 55 °C (Fig. 2b and c). The experiments measured at pH 8.5 and 9.0 Tri-HCl using Mn^{2+} was precipitated (Fig. 2b). Following this, *Sy*Pyk2 activities for PEP were measured under optimal conditions (55 °C and pH 7.0) or intracellular conditions (30 °C and pH 7.8).

Dependence *Sy*Pyk2 cations for catalytic activity

Similar to the other bacterial Pyks (Waygood and Sanwal 1974; Kapoor and Venkitasubramanian 1983; Wu and Turpin 1992; Snášel and Pichová 2019), *Sy*Pyk2 activity was dependent on divalent cations such as Mg^{2+} or Mn^{2+}, and the V_{max} (maximum reaction velocity) of *Sy*Pyk2 activity in the presence of Mn^{2+} was half of that in the presence of Mg^{2+} (Figs. 3, 4a, and b). The activity of *Sy*Pyk2 was higher in the presence of divalent cations than in the presence of monovalent cations, and its activation by monovalent cations was not K^+-specific (Fig. 3). We determined the kinetic parameters of *Sy*Pyk2 with respect to its dependence on Mg^{2+} and Mn^{2+}. Under optimal conditions, the K_m (half-saturation concentration) value of *Sy*Pyk2 for Mg^{2+} and Mn^{2+} dependence was 3.54 ± 0.61 and 0.296 ± 0.02 mM, respectively (Fig. 4a and b). Under intracellular conditions, the K_m value of *Sy*Pyk2 for Mg^{2+} and Mn^{2+} dependence was 6.70 ± 0.26 and 2.18 ± 0.51 mM, respectively (Fig. 4a and

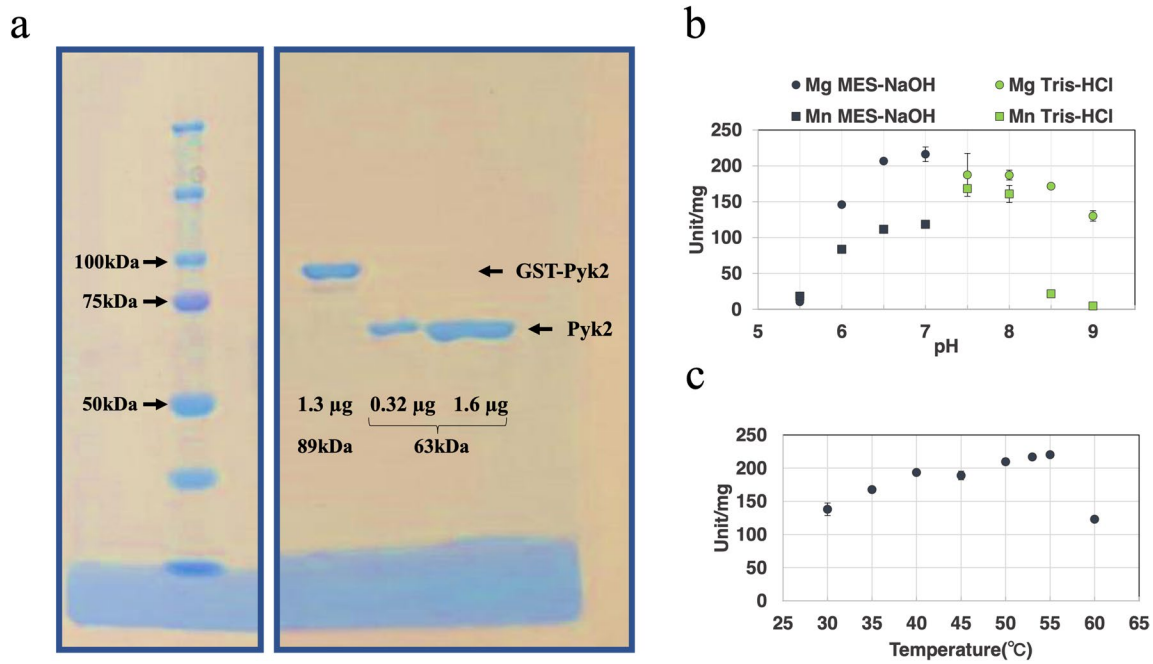

Fig. 2 Sodium dodecyl sulfate–polyacrylamide gel electrophoresis (SDS-PAGE) and optimal pH and temperature for *Synechocystis* pyruvate kinase 2 (*Sy*Pyk2). **a** Purified GST-tagged *Sy*Pyk2 (89 kDa) and untagged *Sy*Pyk2 (63 kDa) proteins. GST-Pyk2 indicated GST-tagged *Sy*Pyk2, and Pyk2 indicated untagged *Sy*Pyk2. The gel was prepared using 8% (w/v) acrylamide and stained with Quick Blue G250. Optimum pH and temperature for *Sy*Pyk2. **b** Effects of the pH on *Sy*Pyk2 activity. The circle and square represented Mg^{2+} and Mn^{2+}, respectively. Blue and green represented the buffer MES-NaOH and Tris–HCl, respectively. The concentrations of phosphoenolpyruvate (PEP), adenosine diphosphate (ADP), and KCl were fixed at 5.0, 2.0, and 100 mM, respectively. The experiments of Mn^{2+} measured at pH 8.5 and 9.0 Tri-HCl was precipitated. The mean ± SD values were calculated from three independent experiments. **c** The effects of temperature on *Sy*Pyk2 activity. This experiment was measured in MES-NaOH buffer pH 7.0, and 15 mM Mg^{2+} of the cofactor was used. PEP, ADP, and KCl concentrations were fixed at 5.0, 2.0, and 100 mM, respectively. The mean ± SD values were calculated from three independent experiments

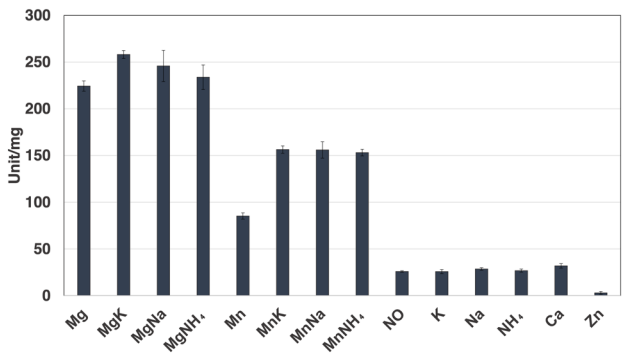

Fig. 3 Effects of cofactor monovalent and divalent cations for *Synechocystis* pyruvate kinase 2 (*Sy*Pyk2) activity. The monovalent and divalent cations were fixed at 100 and 5 mM, respectively, except for $MgCl_2$ and $ZnCl_2$ fixed at 15 and 0.5 mM. The experiment was performed using 100 mM MES-NaOH buffer (pH 7.0) at 55 °C. The concentrations of PEP and ADP were fixed at 5.0 and 2.0 mM, respectively. The mean ± SD values were calculated from three independent experiments. K, KCl; Na, $NaCl_2$; NH_4, NH_4Cl; Mg, $MgCl_2{\cdot}6H_2O$; Mn, $MnCl_2{\cdot}4H_2O$; Ca, $CaCl_2$; Zn, $ZnSO_4{\cdot}7H_2O$

b). The K_m value of *Synechococcus* Pyk and *Synechocystis* PEPC for Mg^{2+} dependence were 2.9 and 4.27 ± 0.46 mM, respectively (Knowles et al. 2001; Scholl et al. 2020). Thus, we defined that the optimum conditions for *Sy*Pyk2 were 15 mM $MgCl_2$ and 5 mM $MnCl_2$.

Determination of kinetic parameters of *Sy*Pyk2

We measured the kinetic parameters of *Sy*Pyk2 for PEP and ADP under optimal conditions. The saturation curves of *Sy*Pyk2 for PEP displayed a sigmoidal curve with V_{max} and K_m of 241 ± 10.5 unit/mg and 1.53 ± 0.07 mM, respectively, and a Hill coefficient of 3.10 ± 0.11, indicating positive homotropic cooperativity (Fig. 5a and Table 1). The saturation curves of *Sy*Pyk2 for ADP followed a hyperbolic (Michaelis–Menten) curve with V_{max} and K_m of 239 ± 6 unit/mg and 0.0527 ± 0.0075 mM, respectively (Fig. 5b and Table 1). The saturation curves of *Sy*Pyk2 for PEP and ADP under intracellular conditions were determined. The saturation curves of *Sy*Pyk2 for PEP showed a sigmoidal curve with V_{max} and K_m of 119 ± 7 unit/mg and 2.54 ± 0.12 mM, respectively, and a Hill coefficient of 2.60 ± 0.18,

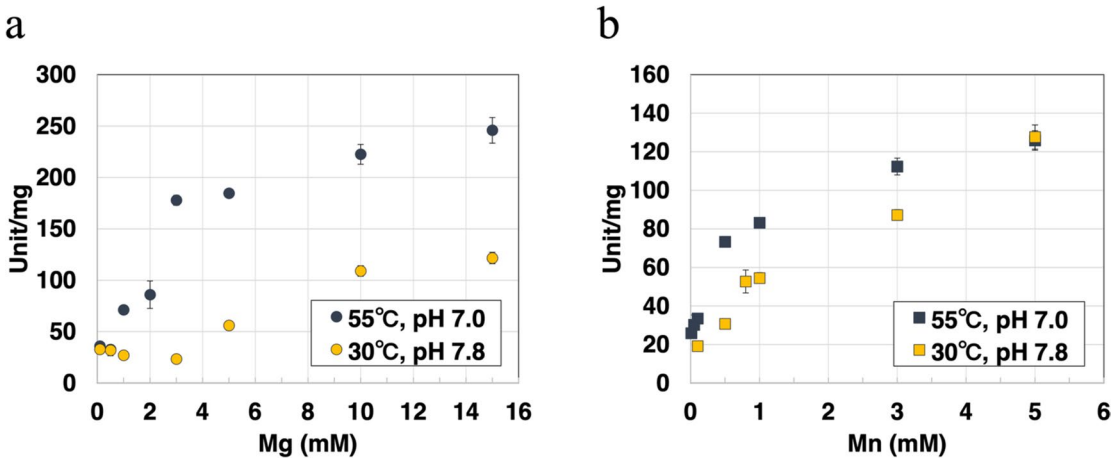

Fig. 4 *Synechocystis* pyruvate kinase 2 (*Sy*Pyk2) activity at different concentrations of $MgCl_2$ (**a**) and $MnCl_2$ (**b**). These experiments were performed under optimum conditions at 55 °C and pH 7.0 in MES-NaOH buffer (blue) or intracellular conditions at 30 °C and pH 7.8 in Tris–HCl buffer (yellow). These experiments fixed the phosphoenolpyruvate (PEP), adenosine diphosphate (ADP), and KCl concentrations at 5.0, 2.0, and 100 mM, respectively. The mean ± SD values were calculated from three independent experiments

suggesting positive homotropic cooperativity (Fig. 5a and Table 1). The saturation curves of *Sy*Pyk2 for ADP exhibited a hyperbolic curve with V_{max} and K_m of 80.3 ± 5.3 Unit/mg and 0.0602 ± 0.0081 mM, respectively (Fig. 5b and Table 1). Similar to *Synechococcus* Pyk and other bacterial Pyks, the saturation curves of *Sy*Pyk2 for PEP showed sigmoidal curves (Knowles et al. 2001; Jetten et al. 1994; Abdelhamid et al. 2019; 2021), and for ADP, hyperbolic curves (Abdelhamid et al. 2019; 2021). Additionally, we measured the activity of *Sy*Pyk2 at 30 °C and pH 7.0; the conditions were optimal for *Synechocystis* PEPC (Takeya et al. 2017) and competed with *Sy*Pyk2 for PEP consumption. The saturation curves of *Sy*Pyk2 for PEP displayed a sigmoidal curve with V_{max} and K_m of 132 ± 5 unit/mg and 2.36 ± 0.2 mM, respectively, and a Hill coefficient of 2.61 ± 0.18, indicating positive homotropic cooperativity and intracellular conditions (Supplemental Fig. 1a and Table 2). The saturation curves of ADP followed a hyperbolic curve with V_{max} and K_m of 123 ± 9 unit/mg and 0.111 ± 0.017 mM, respectively (Supplemental Fig. 1b and Table 2). In these conditions, the K_m value of *Sy*Pyk2 for PEP was approximately 30-, 40-, or 20-fold higher than that of *Sy*Pyk2 for ADP under optimum, intracellular, and optimum for *Synechocystis* PEPC conditions, respectively (Tables 1 and 2). The K_m value of *Sy*Pyk2

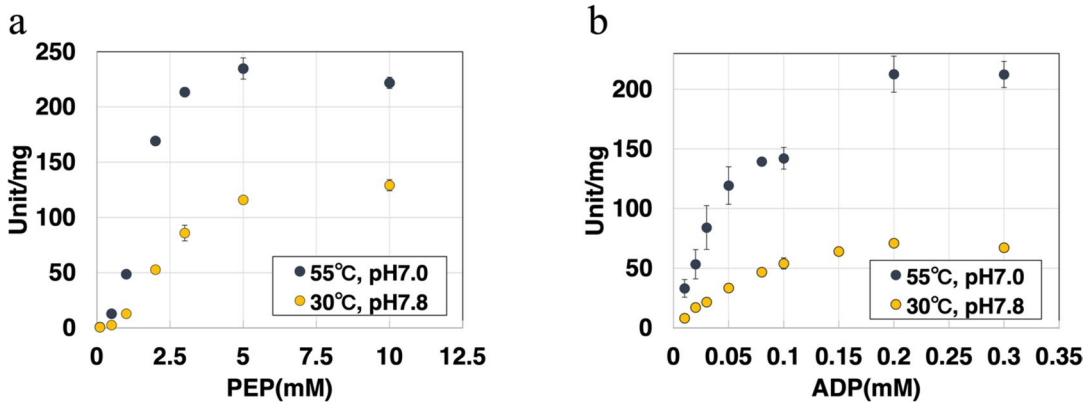

Fig. 5 Saturation curves of *Synechocystis* pyruvate kinase 2 (*Sy*Pyk2) for phosphoenolpyruvate (PEP) and adenosine diphosphate (ADP). **a** The saturation curves of *Sy*Pyk2 for PEP. These measurements were performed in an optimum condition at 55 °C and pH 7.0 in MES-NaOH buffer (blue) or an intracellular condition of 30 °C and pH 7.8 in Tris–HCl (yellow). The ADP concentration was 2.0 mM. The mean ± SD values were calculated from three independent experiments. **b** The saturation curves of *Sy*Pyk2 for ADP. These measurements were performed in an optimum condition at 55 °C and pH 7.0 in MES-NaOH buffer (blue) or an intracellular condition of 30 °C and pH 7.8 in Tris–HCl (yellow). The PEP concentration was 5 mM. The concentrations of KCl and $MgCl_2$ were 100 and 15 mM, respectively. The mean ± SD values were calculated from three independent experiments

Table 1 Kinetic parameters of pyruvate kinase 2 under optimal and intracellular conditions

	V_{max} (Unit/mg)	K_m (mM)	k_{cat} (s^{-1})	k_{cat}/K_m (s^{-1} mM^{-1})	n_H
PEP (55 °C, pH 7.0)	241 ± 10.5	1.53 ± 0.07	253 ± 11	166 ± 3	3.10 ± 0.11
ADP (55 °C, pH 7.0)	238 ± 5	0.0527 ± 0.0076	251 ± 6	4837 ± 733	1.25 ± 0.11
PEP	119 ± 7	2.54 ± 0.118	126 ± 8	49.4 ± 1.2	2.64 ± 0.18
ADP	80.3 ± 5.3	0.0602 ± 0.0081	84.5 ± 5.6	1411 ± 100	1.37 ± 0.24
PEP + ATP	107 ± 5	2.74 ± 0.09	114 ± 5	41.2 ± 0.4	3.06 ± 0.65
PEP + G6P	122 ± 5	0.607 ± 0.009	128 ± 5	212 ± 9	2.00 ± 0.10
PEP + G6P & ATP	130 ± 30	0.62 ± 0.22	137 ± 31	227 ± 25	1.77 ± 0.36
PEP + R5P	125 ± 18	0.548 ± 0.132	131 ± 19	243 ± 29	1.41 ± 0.15
PEP + R5P & ATP	83.0 ± 7.2	0.613 ± 0.100	91.9 ± 7.6	151 ± 10	1.66 ± 0.22

The kinetic parameters of the activity of *Synechocystis* pyruvate kinase 2 (*Sy*Pyk2) in the presence of activators (glucose-6-phosphate, G6P and ribose-5-phosphate, R5P) or inhibitor (adenosine triphosphate, ATP) and coexisting metabolites. All experiments were performed under intracellular conditions of 30 °C and pH 7.8 in Tris–HCl buffer, except for those marked as 55 °C and pH 7.0 in MES-NaOH buffer. Each kinetic parameter is explained as follows: V_{max} (maximum reaction velocity); K_m, half-saturation concentration; k_{cat}, turnover number; k_{cat}/K_m, catalytic efficiency; n_H, Hill coefficient. Mean ± SD values were calculated from three independent experiments

Table 2 Kinetic parameters of *Synechocystis* pyruvate kinase 2 and PEPC under optimal conditions for *Synechocystis* PEPC

	V_{max} (Unit/mg)	K_m (mM)	k_{cat} (s^{-1})	k_{cat}/K_m (s^{-1} mM^{-1})	n_H
PEP (30 °C, pH 7.0)	132 ± 5	2.36 ± 0.20	139 ± 5	59.1 ± 3.1	2.61 ± 0.17
ADP (30 °C, pH 7.0)	123 ± 9	0.111 ± 0.017	130 ± 9	1179 ± 90	0.76 ± 0.04
Synechocystis PEPC (Takeya et al. 2017) (30 °C, pH7.0)	1.74	0.34	na	na	na
Synechocystis PEPC (Scholl et al. 2020) (28 °C, pH 8.0)	24.2 ± 2.30	0.88 ± 0.15	48.71 ± 4.63	na	na

This table shows the kinetic parameters of the activity of *Synechocystis* pyruvate kinase 2 (*Sy*Pyk2) under optimal conditions for *Synechocystis* phosphoenolpyruvate carboxylase (PEPC) at 30 °C and pH 7.0 (Takeya et al. 2017). The experiments *Sy*Pyk2 were performed at 30 °C and pH 7.0 in MES-NaOH buffer. Each kinetic parameter is explained as follows: V_{max} (maximum reaction velocity); K_m, half-saturation concentration; k_{cat}, turnover number; k_{cat}/K_m, catalytic efficiency; n_H, Hill coefficient; na, data not available. The mean ± SD values were calculated from three independent experiments

for ADP was half of that of *Synechococcus* Pyk, and the K_m value of *Sy*Pyk2 for PEP was 5-fold higher than that of *Synechococcus* Pyk (Knowles et al. 2001). Compared with the K_m value of *Synechocystis* PEPC (0.34 mM: Takeya et al. 2017, 0.88 mM: Scholl et al. 2020) for PEP, *Sy*Pyk2 required more than 2-fold PEP (Tables 1 and 2).

Activation and inhibition of *Sy*Pyk2 by sugar phosphates and organic acids

We measured the relative catalytic activity of *Sy*Pyk2 for PEP in the presence of sugar phosphates from the EMP/gluconeogenesis and OPP pathways at 1 mM, and PEP and ADP was fixed at K_m (2.5 mM) and 2 mM respectively, under intracellular conditions. The effectors did not affect LDH (coupled enzyme) used in the experiment. Additionally, several effector metabolites known to inhibit Pyk from the TCA cycle, such as citrate and 2OG, were added at 1 mM under optimum conditions (Wu and Turpin 1992; Knowles et al. 2001). Under optimal conditions, *Sy*Pyk2 was activated by 1 mM G6P and R5P up to 200 and 150%, respectively, and inhibited down to 75% by ATP (Fig. 6). Under intracellular conditions, *Sy*Pyk2 was activated in the presence of 1 mM G6P and R5P by 150 and 125%, respectively, and inhibited in the presence of ATP by up to 75% (Fig. 6). Unlike *Synechococcus* Pyk and green alga, *Chlamydomonas reinhardtii* Pyk, *Sy*Pyk2 was not activated by AMP or F6P and not inhibited by the TCA cycle metabolites, such as citrate, 2OG, and malate (Fig. 6; Wu and Turpin 1992; Knowles et al. 2001).

Furthermore, we calculated the kinetic parameters of *Sy*Pyk2 for PEP in the presence of activators or inhibitors under intracellular conditions. The saturation curves of *Sy*Pyk2 for PEP in the presence of G6P revealed a hyperbolic curve with V_{max} and K_m of 122 ± 5 unit/mg and 0.607 ± 0.01 mM, respectively, and a Hill coefficient

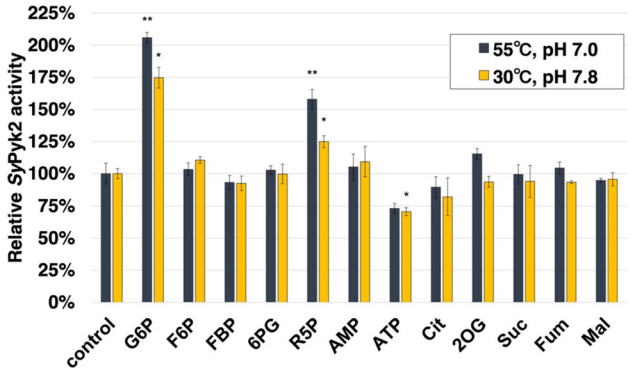

Fig. 6 Effects of effectors for *Synechocystis* pyruvate kinase 2 (*Sy*Pyk2) activity. The effects of various metabolites on the activity *Sy*Pyk2. These experiments measured optimum conditions at 55 °C and pH 7.0 in MES-NaOH buffer (left blue bar) and intracellular conditions at 30 °C and pH 7.8 in Tris–HCl buffer (right yellow bar). The mean ± SD values were calculated from three independent experiments. The concentration of PEP and ADP were fixed at K_m (2.5 mM) and 2.0 mM, respectively. In the measurements of the saturation curves of *Sy*Pyk2, the concentrations of KCl and $MgCl_2$ were 100 and 15 mM, respectively. The concentration of several effectors was 1.0 mM. G6P, glucose-6-phosphate-2Na; F6P, fructose-6-phosphate-2Na; FBP, fructose-1, 6-bisphosphate-3Na; R5P, ribose-5-phosphate-2Na; 6PG, 6-phospho-D-gluconate; AMP, adenosine monophosphate-Na; ADP, adenosine diphosphate-2Na; ATP, adenosine triphosphate-2Na; Cit, citrate-3Na; 2OG, 2-oxoglutarete; Suc, succinate-2Na; Fum: fumarate, Mal: malate-Na. The asterisks indicated significant differences between the absence and presence of the salt (Student's *t*-test; $*P < 0.01$, $**P < 0.005$)

of 2.0 ± 0.1, indicating G6P converting *Sy*Pyk2 from sigmoidal to hyperbolic kinetics (Fig. 7a and Table 1). The enzymatic activities of *Sy*Pyk2 for PEP in the presence of R5P displayed a hyperbolic curve with V_{max} and K_m of 125 ± 18 unit/mg and 0.548 ± 0.132 mM, respectively, and a Hill coefficient of 1.4 ± 0.2, indicating R5P altering *Sy*Pyk2 from sigmoidal to hyperbolic kinetics (Fig. 7a and Table 1). Similar to *Synechococcus* Pyk, G6P and R5P decreased the K_m value of *Sy*Pyk2 for PEP to one-fifth of its value (Knowles et al. 2001 and Table 1). Moreover, the K_m value of *Sy*Pyk2 was increased by ATP from 2.54 to 2.73 mM (Fig. 7b and Table 1). To demonstrate the effects of ATP for *Sy*Pyk2, we calculated the kinetic parameters of *Sy*Pyk2 for PEP in the presence of ATP and either G6P or R5P under intracellular conditions (Fig. 7a and b). G6P, R5P, and ATP concentrations were fixed at 1 mM. The saturation curves of *Sy*Pyk2 for PEP in the presence of ATP and G6P revealed a hyperbolic curve with V_{max} and K_m of 130 ± 29.5 unit/mg and 0.619 ± 0.022 mM, respectively, and a Hill coefficient of 1.73 ± 0.36 (Fig. 7a and b, and Table 1). The enzymatic activities of *Sy*Pyk2 for PEP in the presence of ATP and R5P displayed a hyperbolic curve with V_{max} and K_m of 84.0 ± 7.08 unit/mg and 0.572 ± 0.111 mM, respectively, and a Hill coefficient of 1.89 ± 0.41 (Fig. 7a and b and Table 1). G6P and R5P relieved the effects of ATP (Fig. 7b). Additionally, the IC_{50} (median inhibition concentration) of ATP for *Sy*Pyk2 was 4.1 mM (Supplemental Fig. 2), which was approximately 3-fold higher than that of *Synechococcus* Pyk (1.5 mM, Knowles et al. 2001). G6P and R5P increased the

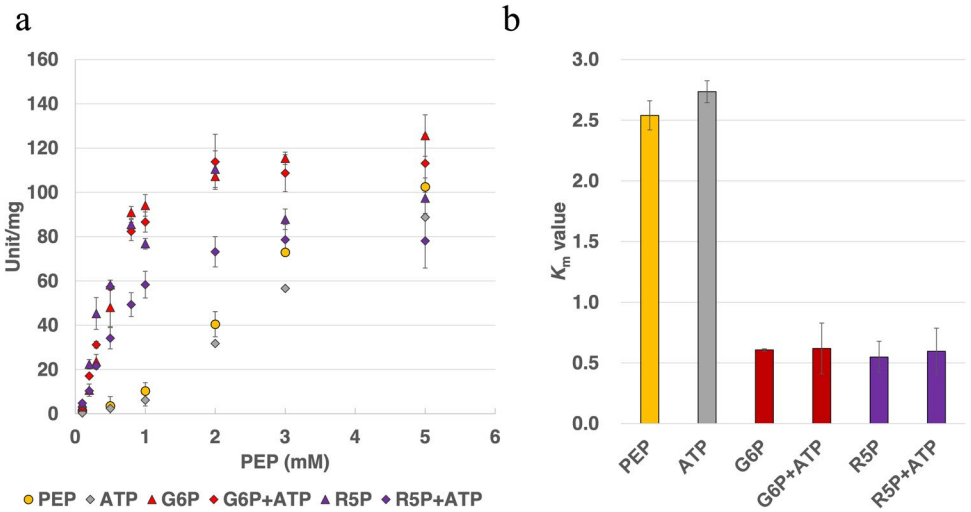

Fig. 7 **a** Influence of several effectors for *Synechocystis* pyruvate kinase 2 (*Sy*Pyk2) activity. Circles (blue) indicated the phosphoenolpyruvate (PEP) saturation curve, squares (red and purple) indicated 1.0 mM of glucose-6-phosphate (G6P) and ribose-5-phosphate (R5P), diamonds (gray) indicated 1.0 mM of adenosine triphosphate (ATP) added, and red or purple diamonds indicated the presence of G6P and R5P with ATP added respectively. The mean ± SD values were calculated from three independent experiments. **b** This figure shows the K_m value of *Sy*Pyk2 for PEP in the presence of G6P, R5P, and ATP, coexisting intracellular conditions of 30 °C and pH 7.8 in Tris–HCl buffer. The mean ± SD values were calculated from three independent experiments

affinity of *Sy*Pyk2 for PEP and remained unaltered in the presence of AMP, F6P, or FBP (Figs. 6, 7a, and b, Table 1).

Discussion

This study demonstrated the properties of *Sy*Pyk2 via biochemical analysis, with G6P and R5P increasing the affinity of *Sy*Pyk2 for PEP *in vitro*. The optimum pH and temperature of Pyks were discovered in bacteria (Chai et al. 2016; Kapoor and Venkitasubramanian 1983; Abbe and Yamada 1982). The optimum pH of Pyks displayed a wide peak range, from acidic to alkaline (Chai et al. 2016; Abbe and Yamada 1982). For *Synechococcus* Pyk, the optimal pH ranged from 6.0 to 7.8, and it was active in the dark (Knowles et al. 2001). The intracellular pH of *Synechocystis* under the photoautotrophic condition was 7.8 (Nakamura et al. 2021), and light to dark transition decreases the intracellular pH of other cyanobacteria from alkaline to neutral (Falkner et al. 1976; Mangan et al. 2016). Thus, the broad pH range of *Sy*Pyk2 indicated that *Sy*Pyk2 could act on PEP consumption under any cultivation conditions. The optimum temperature of *Sy*Pyk2 was 55 °C (Fig. 2c). *Synechocystis* grows at ~ 30 °C (Inoue et al. 2001), and the optimum temperature of *Sy*Pyk2 is higher than that of the cultivation conditions (Fig. 2c). Although for a short time 5 min, *Synechocystis* is viable up to 54 °C (Inoue et al. 2001). Under heat shock conditions, ATP plays a crucial role in protein maintenance through chaperones (Soini et al. 2005). The gene expression of *pyk2* increases during heat shocks (Slabas et al. 2006), and hence, *Sy*Pyk2 may contribute to ATP production by increasing its enzymatic activity.

Pyks have been studied for their properties and primary sequences (Hunsley and Suelter 1969; Cottam et al. 1969; Abdelhamid et al. 2019; 2021). All Pyks require divalent cations, such as Mg^{2+} or Mn^{2+}, and numerous Pyks require K^+ for activity (Baek and Nowak 1982; Kachmar and Boyer 1953). *Sy*Pyk2 showed Mg^{2+}- and Mn^{2+}-dependent activity and other bacterial Pyks, and its activity was stimulated by monovalent cations, such as K^+, Na^+, or NH_4^+(Fig. 3). Bacterial Pyks are classified into two types: PykA, which is stimulated by sugar monophosphates, such as AMP, G6P, and R5P, and PykF, activated by sugar diphosphates, such as FBP in *E. coli* (Kornberg and Malcovati 1973; Waygood et al. 1975, 1976). Moreover, *Sy*Pyk2 is classified as PykF (Kaneko et al. 1996). In silico analysis suggests that two isozymes, Pyk1 and Pyk2 have the same allosteric sites for G6P, R5P, FBP, AMP, and ATP (Haghighi 2021). Pyks containing Pyk1 and Pyk2 from *Synechocystis* cells are activated by G6P, F6P, R5P, and AMP but not by FBP (Knowles and Plaxton 2003). Based on these findings, we demonstrated the regulation of *Sy*Pyk2 by adding various metabolites from the OPP pathway, EMP/gluconeogenesis pathway, and TCA cycle (Fig. 7a). Our findings reveal a decrease in the K_m value of *Sy*Pyk2 with K-type characteristics, indicative of altered substrate affinity and allosteric activation by G6P and R5P (Fig. 7b and Table 1). Our results suggest that G6P and R5P may also activate *Sy*Pyk1. Therefore, *Sy*Pyk2 is dependent on divalent cations, such as Mg^{2+} and Mn^{2+}, and is classified as PykA type rather than PykF, stimulated by sugar monophosphates, such as G6P and R5P, but not by AMP.

The K_m values of *Sy*Pyk2 for PEP were 40-fold higher than ADP, indicating a higher requirement for PEP in its enzymatic reaction than ADP under intracellular conditions (Table 1). The K_m value of *Synechococcus* Pyk for PEP is higher than that for ADP (Knowles et al. 2001). The K_m value of *Sy*Pyk2 for PEP is higher than *Synechococcus* Pyk 5-fold (Table 1 and Knowles et al. 2001). Additionally, the absolute concentration of ADP in *Synechocystis* cells is three times higher than that of PEP (Dempo et al. 2014). These data indicate that these two Pyk enzymes, *Synechocystis* and *Synechococcus*, are limited by PEP concentration in their reactions under photosynthetic conditions. However, its mechanism is different. *Synechococcus* Pyk has high PEP affinity and allosteric inhibition by citrate and ATP (Knowles et al. 2001). *Synechocystis* has a low affinity and not inhibited by either citrate or ATP (Table 1 and Fig. 6). Thus, these findings suggested that the availability of PEP limited the enzymatic activity of *Sy*Pyk2 for the flux of PEP to pyruvate via *Sy*Pyk2 under photosynthetic conditions.

Rapid glycogen catabolism induces glucan polymer such as G6P and signaling metabolites such as 2OG occur during nitrogen depletion (Joseph et al. 2014), indicating that G6P may activate *Sy*Pyk2. Although *Synechococcus* Pyk is repressed by 2OG, *Sy*Pyk2 is not (Fig. 6). However, a previous study reveals that *pyk1* expression is induced 3.5-fold, and *pyk2* expression is reduced by half during nitrogen-deficient conditions (Osanai et al. 2006). Hence, these findings indicate that to provide a carbon source to the TCA cycle for 2OG production, *Sy*Pyk2 may act during the initial stages of nitrogen depletion through G6P and R5P activation and then be replaced with *Sy*Pyk1. Furthermore, *pyk1* is regulated by several nitrogen-related regulators such as SigE, Rre37 thorough with NtcA (Giner-Lamia et al. 2017; Iijima et al. 2014; Osanai et al. 2005). Therefore, in *Synechocystis*, we consider *Sy*Pyk1 and *Sy*Pyk2 to mainly function as pyruvate kinase during the late and initial nitrogen depletion stages, respectively.

In comparison to the K_m value of PEP for *Synechocystis* PEPC (0.34 mM: Takeya et al. 2017; 0.88 mM: Scholl et al. 2020 and Table 2), *Sy*Pyk2 (2.54 mM, Table 1) required more than 2-fold higher concentration of PEP (Tables 1 and 2). The K_m value of *Sy*Pyk2 for PEP was decreased from

2.54 to 0.607 or 0.548 mM by G6P or R5P, respectively (Fig. 7a and b and Table 1). The higher PEP requirement and the enhanced affinity of *Sy*Pyk2 for PEP by G6P and R5P, suggesting a role for *Sy*Pyk2 in *Synechocystis* cells. In a previous study, Pyk from *Synechocystis* demonstrated a higher Pyk activity under heterotrophic conditions than under photoautotrophic and mixotrophic conditions (Knowles and Plaxton 2003). Recently, ME, which generates pyruvate from malate by the ME-dependent TCA cycle, was reportedly active under photoautotrophic conditions (Katayama et al. 2022), indicating that pyruvate is synthesized by ME and not by Pyk (Bricker et al. 2004; Qian et al. 2018). The pathway involving PEPC, MDH, and ME constitutes an alternate route for pyruvate formation in *Synechocystis* cells under photosynthetic conditions (You et al. 2014; Bricker et al. 2004). ATP functions as an inhibitor of *Synechococcus* Pyk, which is the homolog of *Sy*Pyk2 (Knowles et al. 2001). This observation suggests that the lack of Pyk flux under photosynthetic conditions can be attributed to ATP inhibition (Bricker et al. 2004). In *E. coli*, the intracellular concentration of ATP is suggested to be 0.6 mM (Boecker et al. 2019) and not much different from *Synechocystis* (Wan et al. 2017). G6P and ATP exhibit comparable concentrations, approximately $1.84*10^{0}$ and $2.14*10^{0}$ µmol/g-dry cell weight, respectively (Dempo et al. 2014). R5P is one-tenth of the concentration of ATP, amounting to $1.95*10^{-1}$ µmol/g-dry cell (Dempo et al. 2014). Hence, to demonstrate the in vivo effects of metabolites, we maintained uniform effector concentrations at 1 mM. Inhibition by 1 mM ATP decreased the V_{max} and increased the K_m value of *Sy*Pyk2 activity (Table 1 and Fig. 7b). The V_{max} of *Sy*Pyk2 for PEP decreased from 119 ± 7 to 107 ± 5, and the K_m value of *Sy*Pyk2 for PEP increased from 2.54 to 2.74 mM (1.07-fold) (Fig. 7b and Table 1). In comparison, the K_m value of *Synechococcus* Pyk increased from 0.54 to 0.75 mM (1.37-fold) by 0.5 mM ATP (Knowles et al. 2001). Furthermore, compared to the IC_{50} of *Synechococcus* Pyk for ATP (1.5 mM: Knowles et al. 2001), *Sy*Pyk2 (4.1 mM: Supplemental Fig. 2) was approximately 3-fold higher, indicating that *Sy*Pyk2 is less affected by ATP than *Synechococcus* Pyk. Additionally, the presence of G6P and R5P alleviated the inhibitory effects of ATP, reducing the K_m value of the substrate concentration to approximately one-fifth (Fig. 7a and b). Our results showed that the effects of ATP on *Sy*Pyk2 are less potent than those of G6P and R5P. Considering the IC_{50} and the slight increase in the K_m value by ATP, it suggests that *Sy*Pyk2 is less influenced by ATP. Therefore, we conclude that the low flux of PEP to pyruvate via Pyk is due to its extremely low affinity for PEP (Tables 1 and 2; Knowles et al. 2001) and the absence of activators such as G6P and R5P under photosynthetic conditions.

The flux through the OPP pathway increases under nonphotosynthetic conditions (Wan et al. 2017) relative to photosynthetic conditions (Young et al. 2011), indicating a significant elevation in the levels of G6P and R5P under nonphotosynthetic conditions. Moreover, PEP increases and decreases under photosynthetic and nonphotosynthetic conditions, respectively (Werner et al. 2019). Consequently, the accumulation of G6P and R5P under nonphotosynthetic conditions upregulates the *Sy*Pyk2 reaction. Following *Sy*Pyk2 activation in the presence of G6P and R5P, PEP is consumed by *Sy*Pyk2, alleviating glucose-6-phosphate dehydrogenase (G6PDH encoded by *zwf*, slr1843) inhibition, a rate-limiting enzyme of the OPP pathway (Ito and Osanai 2020). Furthermore, PEP consumption via *Sy*Pyk2 activating relieving the inhibition of 6-phosphogluconate dehydrogenase (6PGDH encoded by *gnd*, sll0329) (Ito and Osanai, 2018), an enzyme involved in the third reaction of the OPP pathway (Fig. 8). In this feedforward regulation, *Sy*Pyk2 primarily acts as relieving the sugar catabolic repression under nonphotosynthetic conditions.

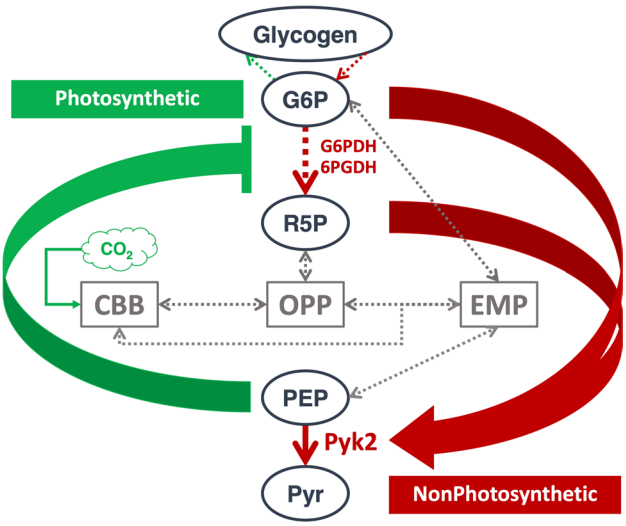

Fig. 8 Model of glucose-6-phosphate (G6P), ribose-5-phosphate (R5P) and phosphoenolpyruvate (PEP) regulation of carbon flow under photosynthetic or nonphotosynthetic conditions in *Synechocystis*sp. PCC 6803. EMP, Embden–Meyerhof–Parnas pathway; OPP, oxidative pentose phosphate pathway; CBB, Calvin Benson Bassham cycle; Pyr, pyruvate; G6PDH, glucose-6-phosphate dehydrogenase; 6PGDH, 6-phosphogluconate dehydrogenase; Pyk2, pyruvate kinase 2

This study offers valuable insights into the biosynthesis and fermentation of metabolites associated with pyruvate metabolism, particularly PEP consumption in *Synechocystis*.

This study demonstrated that the regulation of *Sy*Pyk2 is dependent on PEP accumulation, the presence of G6P, R5P, and divalent cations, such as Mg^{2+} and Mn^{2+}, rather than pH and ATP. Therefore, our experiments indicated that *Sy*Pyk2 contributed less to PEP consumption under

photosynthetic conditions and that it plays a pivotal role in sugar catabolism under nonphotosynthetic conditions in response to sugar phosphate accumulation.

Supplementary Information The online version contains supplementary material available at https://doi.org/10.1007/s11103-023-01401-0.

Author contributions MK designed the study, performed the experiments, analyzed the data, and wrote the manuscript. NK analyzed the data. TO analyzed the data and wrote the manuscript.

Funding Open Access funding provided by Meiji University. This work was supported by the following grants to TO: JSPS KAKENHI Grant-in-Aid for Scientific Research (B) (Grant Number 20H02905) and JST-ALCA of the Japan Science and Technology Agency (Grant Number JPMJAL1306).

Data availability Not applicable.

Declarations

Competing interest The authors declare no competing interests.

References

Abbe K, Yamada T (1982) Purification and properties of pyruvate kinase from *Streptococcus mutans*. J Bacteriol 149:299–305. https://doi.org/10.1128/jb.149.1.299-305.1982

Abdelhamid Y, Brear P, Greenhalgh J, Chee X, Rahman T, Welch M (2019) Evolutionary plasticity in the allosteric regulator-binding site of pyruvate kinase isoform PykA from *Pseudomonas aeruginosa*. J Biol Chem 294:15505–15516. https://doi.org/10.1074/jbc.RA119.009156

Abdelhamid Y, Wang M, Parkhill SL, Brear P, Chee X, Rahman T, Welch M (2021) Structure, function and regulation of a second pyruvate kinase isozyme in *Pseudomonas aeruginosa*. Front Microbiol 12:790742. https://doi.org/10.3389/fmicb.2021.790742

Abernathy MH, Yu J, Ma F, Liberton M, Ungerer J, Hollinshead WD, Gopalakrishnan S, He L, Maranas CD, Pakrasi HB, Allen DK, Tang YJ (2017) Deciphering cyanobacterial phenotypes for fast photoautotrophic growth via isotopically nonstationary metabolic flux analysis. Biotechnol Biofuels 10:273. https://doi.org/10.1186/s13068-017-0958-y

Allison W, Corey DB, Ashok P, Christie AMP (2019) A comprehensive time-course metabolite profiling of the model cyanobacterium Synechocystis sp. PCC 6803 under diurnal light:dark cycles

Angermayr SA, van der Woude AD, Correddu D, Vreugdenhil A, Verrone V, Hellingwerf KJ (2014) Exploring metabolic engineering design principles for the photosynthetic production of lactic acid by *Synechocystis* sp. PCC6803. Biotechnol Biofuels 7:99. https://doi.org/10.1186/1754-6834-7-99

Baek YH, Nowak T (1982) Kinetic evidence for a dual cation role for muscle pyruvate kinase. Arch Biochem Biophys 217:491–497. https://doi.org/10.1016/0003-9861(82)90529-x

Boecker S, Zahoor A, Schramm T, Link H, Klamt S (2019) Broadening the scope of enforced ATP wasting as a tool for metabolic engineering in *Escherichia coli*. Biotechnol J 14:1800438. https://doi.org/10.1002/biot.201800438

Bricker TM, Zhang S, Laborde SM, Mayer PR 3rd, Frankel LK, Moroney JV (2004) The malic enzyme is required for optimal photoautotrophic growth of *Synechocystis* sp. strain PCC 6803 under continuous light but not under a diurnal light regimen. J Bacteriol 186:8144–8148. https://doi.org/10.1128/JB.186.23.8144-8148

Carpine R, Du W, Olivieri G, Pollio A, Hellingwerf KJ, Marzocchella A, dos Santos FB (2017) Genetic engineering of *Synechocystis* sp. PCC6803 for poly-β-hydroxybutyrate overproduction. Algal Res 25:117–127. https://doi.org/10.1016/j.algal.2017.05.013

Chai X, Shang X, Zhang Y, Liu S, Liang Y, Zhang Y, Wen T (2016) A novel pyruvate kinase and its application in lactic acid production under oxygen deprivation in *Corynebacterium glutamicum*. BMC Biotechnol 16:79. https://doi.org/10.1186/s12896-016-0313-6

Cooley JW, Vermaas WF (2001) Succinate dehydrogenase and other respiratory pathways in thylakoid membranes of *Synechocystis* sp. strain PCC 6803: capacity comparisons and physiological function. J Bacteriol 183:4251–4258. https://doi.org/10.1128/JB.183.14.4251-4258.2001

Cottam GL, Hollenberg PF, Coon MJ (1969) Subunit structure of rabbit muscle pyruvate kinase. J Biol Chem 244:1481–1486. https://doi.org/10.1016/S0021-9258(18)91785-0

de Alvarenga LV, Hess WR, Hagemann M (2020) AcnSP—a novel small protein regulator of aconitase activity in the cyanobacterium *Synechocystis* sp. PCC 6803. Front Microbiol 11:1445. https://doi.org/10.3389/fmicb.2020.01445

Dempo Y, Ohta E, Nakayama Y, Bamba T, Fukusaki E (2014) Molar-based targeted metabolic profiling of cyanobacterial strains with potential for biological production. Metabolites 4:499–516. https://doi.org/10.3390/metabo4020499

Falkner G, Horner F, Werdan K, Heldt H (1976) Concomitant changes in phosphate uptake and photophosphorylation in the blue-green *Alga Anacystis* nidulans during adaptation to phosphate deficiency. Plant Physiol 58:717–718. https://doi.org/10.1016/S0176-1617(11)80928-4

Giner-Lamia J, Robles-Rengel R, Hernández-Prieto MA, Muro-Pastor MI, Florencio FJ, Futschik ME (2017) Identification of the direct regulon of NtcA during early acclimation to nitrogen starvation in the cyanobacterium *Synechocystis* sp. PCC 6803. Nucleic Acids Res 45:11800–11820. https://doi.org/10.1093/nar/gkx860

Guerrero-Mendiola C, García-Trejo JJ, Encalada R, Saavedra E, Ramírez-Silva L (2017) The contribution of two isozymes to the pyruvate kinase activity of *Vibrio cholerae*: one K^+-dependent constitutively active and another K^+-independent with essential allosteric activation. PLoS ONE 12:e0178673. https://doi.org/10.1371/journal.pone.0178673

Haghighi O (2021) In silico study of the structure and ligand preference of pyruvate kinases from cyanobacterium *Synechocystis* sp. PCC 6803. Appl Biochem Biotechnol 193:3651–3671. https://doi.org/10.1007/s12010-021-03630-9

Hasunuma T, Matsuda M, Kondo A (2016) Improved sugar-free succinate production by *Synechocystis* sp. PCC 6803 following identification of the limiting steps in glycogen catabolism. Metab Eng Commun 3:130–141. https://doi.org/10.1016/j.meteno.2016.04.003

Hasunuma T, Matsuda M, Kato Y, Vavricka CJ, Kondo A (2018) Temperature enhanced succinate production concurrent with increased central metabolism turnover in the cyanobacterium *Synechocystis* sp. PCC 6803. Metab Eng 48:109–120. https://doi.org/10.1016/j.ymben.2018.05.013

Hauf W, Schlebusch M, Hüge J, Kopka J, Hagemann M, Forchhammer K (2013) Metabolic changes in *Synechocystis* PCC6803 upon nitrogen-starvation: excess NADPH sustains polyhydroxybutyrate accumulation. Metabolites 3:101–118. https://doi.org/10.3390/metabo3010101

Hidese R, Matsuda M, Osanai T, Hasunuma T, Kondo A (2020) Malic enzyme facilitates D-lactate production through increased pyruvate supply during anoxic dark fermentation in *Synechocystis* sp. PCC 6803. ACS Synth Biol 9:260–268. https://doi.org/10.1021/acssynbio.9b00281

Hunsley JR, Suelter CH (1969) Yeast pyruvate kinase. I: purification and some chemical properties. J Biol Chem 244:4815–4818. https://doi.org/10.1016/S0021-9258(18)94276-6

Iijima H, Watanabe A, Takanobu J, Hirai MY, Osanai T (2014) rre37 overexpression alters gene expression related to the tricarboxylic acid cycle and pyruvate metabolism in *Synechocystis* sp. PCC 6803. Sci World J 2014:921–976. https://doi.org/10.1155/2014/921976

Inoue N, Taira Y, Emi T, Yamane Y, Kashino Y, Koike H, Satoh K (2001) Acclimation to the growth temperature and the high-temperature effects on photosystem II and plasma membranes in a mesophilic cyanobacterium, *Synechocystis* sp. PCC6803. Plant Cell Physiol 42:1140–1148. https://doi.org/10.1093/pcp/pce147

Ito S, Osanai T (2018) Single amino acid change in 6-phosphogluconate dehydrogenase from *Synechocystis* conveys higher affinity for $NADP^+$ and altered mode of inhibition by NADPH. Plant Cell Physiol 59:2452–2461. https://doi.org/10.1093/pcp/pcy165

Ito S, Osanai T (2020) Unconventional biochemical regulation of the oxidative pentose phosphate pathway in the model cyanobacterium Synechocystis sp. PCC 6803. Biochem J 477(1309–1321): https://doi.org/10.1042/BCJ20200038

Ito S, Takeya M, Osanai T (2017) Substrate specificity and allosteric regulation of a D-Lactate dehydrogenase from a unicellular cyanobacterium are altered by an amino acid substitution. Sci Rep 7:15052. https://doi.org/10.1038/s41598-017-15341-5

Ito S, Koyama N, Osanai T (2019) Citrate synthase from *Synechocystis* is a distinct class of bacterial citrate synthase. Sci Rep 9:6038. https://doi.org/10.1038/s41598-019-42659-z

Jazmin LJ, Xu Y, Cheah YE, Adebiyi AO, Johnson CH, Young JD (2017) Isotopically nonstationary ^{13}C flux analysis of cyanobacterial isobutyraldehyde production. Metab Eng 42:9–18. https://doi.org/10.1016/j.ymben.2017.05.001

Jetten MS, Gubler ME, Lee SH, Sinskey AJ (1994) Structural and functional analysis of pyruvate kinase from *Corynebacterium glutamicum*. Appl Environ Microbiol 60:2501–2507. https://doi.org/10.1128/aem.60.7.2501-2507.1994

Joseph A, Aikawa S, Sasaki K, Teramura H, Hasunuma T, Matsuda F, Osanai T, Hirai MY, Kondo A (2014) Rre37 stimulates accumulation of 2-oxoglutarate and glycogen under nitrogen starvation in *Synechocystis* sp. PCC 6803. FEBS Lett 588:466–471. https://doi.org/10.1016/j.febslet.2013.12.008

Kachmar JF, Boyer PD (1953) Kinetic analysis of enzyme reactions, II: the potassium activation and calcium inhibition of pyruvic phosphoferase. J Biol Chem 200:669–682. https://doi.org/10.1016/S0021-9258(18)71413-0

Kaneko T, Sato S, Kotani H, Tanaka A, Asamizu E, Nakamura Y, Miyajima N, Hirosawa M, Sugiura M, Sasamoto S, Kimura T, Hosouchi T, Matsuno A, Akiko M, Nakazaki N, Naruo K, Okumura S, Shimpo S, Takeuchi C, Wada T, Watanabe A, Yamada M, Yasuda M, Tabata S (1996) Sequence analysis of the genome of the unicellular cyanobacterium *Synechocystis* sp. Strain PCC6803. ii. Sequence determination of the entire genome and assignment of potential protein-coding regions (supplement). DNA Res 3:185–209. https://doi.org/10.1093/dnares/3.3.185

Kaniya Y, Kizawa A, Miyagi A, Kawai-Yamada M, Uchimiya H, Kaneko Y, Nishiyama Y, Hihara Y (2013) Deletion of the transcriptional regulator cyAbrB2 deregulates primary carbon metabolism in *Synechocystis* sp. PCC 6803. Plant Physiol 162:1153–1163. https://doi.org/10.1104/pp.113.218784

Kapoor R, Venkitasubramanian TA (1983) Purification and properties of pyruvate kinase from *Mycobacterium smegmatis*. Arch Biochem Biophys 225:320–330. https://doi.org/10.1016/0003-9861(83)90036-X

Katayama N, Iwazumi K, Suzuki H, Osanai T, Ito S (2022) Malic enzyme, not malate dehydrogenase, mainly oxidizes malate that originates from the tricarboxylic acid cycle in cyanobacteria. Mbio 13:e0218722. https://doi.org/10.1128/mbio.02187-22

Kayne FJ (1973) 11 pyruvate kinase. Enzymes 8:353–382. https://doi.org/10.1016/S1874-6047(08)60071-2

Knoop H, Zilliges Y, Lockau W, Steuer R (2010) The metabolic network of *Synechocystis* sp. PCC 6803: systemic properties of autotrophic growth. Plant Physiol 154:410–422. https://doi.org/10.1104/pp.110.157198

Knowles VL, Plaxton WC (2003) From genome to enzyme: analysis of key glycolytic and oxidative pentose-phosphate pathway enzymes in the cyanobacterium *Synechocystis* sp. PCC 6803. Plant Cell Physiol 44:758–763. https://doi.org/10.1093/pcp/pcg086

Knowles VL, Smith CS, Smith CR, Plaxton WC (2001) Structural and regulatory properties of pyruvate kinase from the cyanobacterium *Synechococcus* PCC 6301. J Biol Chem 276:20966–20972. https://doi.org/10.1074/jbc.M008878200

Kornberg HL, Malcovati M (1973) Control in situ of the pyruvate kinase activity of *Escherichia coli*. FEBS Lett 32:257–259. https://doi.org/10.1016/0014-5793(73)80846-4

Mangan NM, Flamholz A, Hood RD, Milo R, Savage DF (2016) pH determines the energetic efficiency of the cyanobacterial CO_2 concentrating mechanism. Proc Natl Acad Sci USA 113:E5354–E5362. https://doi.org/10.1073/pnas.1525145113

Muro-Pastor MI, Florencio FJ (1992) Purification and properties of NADP-isocitrate dehydrogenase from the unicellular cyanobacterium *Synechocystis* sp. PCC 6803. Eur J Biochem 203:99–105. https://doi.org/10.1111/j.1432-1033.1992.tb19833.x

Nakajima T, Kajihata S, Yoshikawa K, Matsuda F, Furusawa C, Hirasawa T, Shimizu H (2014) Integrated metabolic flux and omics analysis of *Synechocystis* sp. PCC 6803 under mixotrophic and photoheterotrophic conditions. Plant Cell Physiol 55:1605–1612. https://doi.org/10.1093/pcp/pcu091

Nakamura S, Fu N, Kondo K, Wakabayashi K, Hisabori T, Sugiura K (2021) A luminescent Nanoluc-GFP fusion protein enables readout of cellular pH in photosynthetic organisms. J Biol Chem 296:100134. https://doi.org/10.1074/jbc.RA120.016847

Nishii M, Ito S, Katayama N, Osanai T (2021) Biochemical elucidation of citrate accumulation in *Synechocystis* sp. PCC 6803 via kinetic analysis of aconitase. Sci Rep 11:17131. https://doi.org/10.1038/s41598-021-96432-2

Osanai T, Kanesaki Y, Nakano T, Takahashi H, Asayama M, Shirai M, Kanehisa M, Suzuki I, Murata N, Tanaka K (2005) Positive regulation of sugar catabolic pathways in the cyanobacterium *Synechocystis* sp. PCC 6803 by the group 2 σ factor SigE. J Biol Chem 280:30653–30659. https://doi.org/10.1074/jbc.M505043200

Osanai T, Imamura S, Asayama M, Shirai M, Suzuki I, Murata N, Tanaka K (2006) Nitrogen induction of sugar catabolic gene expression in *Synechocystis* sp. PCC 6803. DNA Res 13:185–195. https://doi.org/10.1093/dnares/dsl010

Osanai T, Oikawa A, Shirai T, Kuwahara A, Iijima H, Tanaka K, Ikeuchi M, Kondo A, Saito K, Hirai MY (2013) Capillary electrophoresis–mass spectrometry reveals the distribution of carbon

metabolites during nitrogen starvation in *Synechocystis* sp. PCC 6803. Environ Biol 16:512–524. https://doi.org/10.1111/1462-2920.12170

Osanai T, Shirai T, Iijima H, Nakaya Y, Okamoto M, Kondo A, Hirai MY (2015) Genetic manipulation of a metabolic enzyme and a transcriptional regulator increasing succinate excretion from unicellular cyanobacterium. Front Microbiol 6:1064. https://doi.org/10.3389/fmicb.2015.01064

Qian X, Zhang Y, Lun DS, Dismukes GC (2018) Rerouting of metabolism into desired cellular products by nutrient stress: fluxes reveal the selected pathways in cyanobacterial photosynthesis. ACS Synth Biol 7:1465–1476. https://doi.org/10.1021/acssynbio.8b00116

Ruffing AM (2011) Engineered cyanobacteria: teaching an old bug new tricks. Bioeng Bugs 2:136–149. https://doi.org/10.4161/bbug.2.3.15285

Saha R, Liu D, Hoynes-O'Connor A, Liberton M, Yu J, Bhattacharyya-Pakrasi M, Balassy A, Zhang F, Moon TS, Maranas CD, Pakrasi HB (2016) Diurnal regulation of cellular processes in the cyanobacterium *Synechocystis* sp. strain PCC 6803: insights from transcriptomic, fluxomic, and physiological analyses. Mbio. https://doi.org/10.1128/mBio.00464-16

Sakai H, Suzuki K, Imahori K (1986) Purification and properties of pyruvate kinase from *Bacillus stearothermophilus*. J Biochem 99:1157–1167. https://doi.org/10.1093/oxfordjournals.jbchem.a135579

Scholl J, Dengler L, Bader L, Forchhammer K (2020) Phosphoenolpyruvate carboxylase from the cyanobacterium *Synechocystis* sp. PCC 6803 is under global metabolic control by PII signaling. Mol Microbiol 114:292–307. https://doi.org/10.1111/mmi.14512

Slabas AR, Suzuki I, Murata N, Simon WJ, Hall JJ (2006) Proteomic analysis of the heat shock response in *Synechocystis* PCC6803 and a thermally tolerant knockout strain lacking the histidine kinase 34 gene. Proteomics 6:845–864. https://doi.org/10.1002/pmic.200500196

Snášel J, Pichová I (2019) Allosteric regulation of pyruvate kinase from *Mycobacterium tuberculosis* by metabolites. Biochim Biophys Acta Proteins Proteom 1867:125–139. https://doi.org/10.1016/j.bbapap.2018.11.002

Soini J, Falschlehner C, Mayer C, Böhm D, Weinel S, Panula J, Vasala A, Neubauer P (2005) Transient increase of ATP as a response to temperature up-shift in *Escherichia coli*. Microb Cell Factories 4:9. https://doi.org/10.1186/1475-2859-4-9

Takahashi H, Uchimiya H, Hihara Y (2008) Difference in metabolite levels between photoautotrophic and photomixotrophic cultures of *Synechocystis* sp. PCC 6803 examined by capillary electrophoresis electrospray ionization mass spectrometry. J Exp Bot 59:3009–3018. https://doi.org/10.1093/jxb/ern157

Takeya M, Hirai MY, Osanai T (2017) Allosteric inhibition of phosphoenolpyruvate carboxylases is determined by a single amino acid residue in cyanobacteria. Sci Rep 7:41080. https://doi.org/10.1038/srep41080

Takeya M, Ito S, Sukigara H, Osanai T (2018) Purification and characterisation of malate dehydrogenase from *Synechocystis* sp. PCC 6803: biochemical barrier of the oxidative tricarboxylic acid cycle. Front Plant Sci 9:947. https://doi.org/10.3389/fpls.2018.00947

Tanaka K, Shirai T, Vavricka CJ, Matsuda M, Kondo A, Hasunuma T (2023) Dark accumulation of downstream glycolytic intermediates initiates robust photosynthesis in cyanobacteria. Plant Physiol 191:2400–2413. https://doi.org/10.1093/plphys/kiac602

Wan N, DeLorenzo DM, He L, You L, Immethun CM, Wang G, Baidoo EEK, Hollinshead W, Keasling JD, Moon TS, Tang YJ (2017) Cyanobacterial carbon metabolism: fluxome plasticity and oxygen dependence. Biotechnol Bioeng 114:1593–1602. https://doi.org/10.1002/bit.26287

Wang B, Wang J, Zhang W, Meldrum DR (2012) Application of synthetic biology in cyanobacteria and algae. Front Microbiol. https://doi.org/10.3389/fmicb.2012.00344

Waygood EB, Sanwal BD (1974) The control of pyruvate kinases of *Escherichia coli.* I: physicochemical and regulatory properties of the enzyme activated by fructose 1,6-diphosphate. J Biol Chem 249:265–274. https://doi.org/10.1016/S0021-9258(19)43120-7

Waygood EB, Rayman MK, Sanwal BD (1975) The control of pyruvate kinases of *Escherichia coli*. II: effectors and regulatory properties of the enzyme activated by ribose 5-phosphate. Can J Biochem 53:444–454. https://doi.org/10.1139/o75-061

Waygood EB, Mort JS, Sanwal BD (1976) The control of pyruvate kinase of *Escherichia coli*: binding of substrate and allosteric effectors to the enzyme activated by fructose 1,6-bisphosphate. Biochem 15:277–282. https://doi.org/10.1021/bi00647a006

Werner A, Broeckling CD, Prasad A, Peebles CAM (2019) A comprehensive time-course metabolite profiling of the model cyanobacterium Synechocystis sp. PCC 6803 under diurnal light: dark cycles. Plant J 99:379–388. https://doi.org/10.1111/tpj.14320

Wu HB, Turpin DH (1992) Purification and characterization of pyruvate kinase from the green alga *Chlamydomonas reinhardtii*. J Phycol 28:472–481. https://doi.org/10.1111/j.0022-3646.1992.00472.x

Xiong W, Brune D, Vermaas WF (2014) The γ-aminobutyric acid shunt contributes to closing the tricarboxylic acid cycle in *Synechocystis* sp. PCC 6803. Mol Microbiol 93:786–796. https://doi.org/10.1111/mmi.12699

Yao L, Shabestary K, Björk SM, Asplund-Samuelsson J, Joensson HN, Jahn M, Hudson EP (2020) Pooled CRISPRi screening of the cyanobacterium *Synechocystis* sp PCC 6803 for enhanced industrial phenotypes. Nat Commun 11:1666. https://doi.org/10.1038/s41467-020-15491-7

You L, Berla B, He L, Pakrasi HB, Tang YJ (2014) ^{13}C-MFA delineates the photomixotrophic metabolism of *Synechocystis* sp. PCC 6803 under light- and carbon-sufficient conditions. Biotechnol J 9:684–692. https://doi.org/10.1002/biot.201300477

Young JD, Shastri AA, Stephanopoulos G, Morgan JA (2011) Mapping photoautotrophic metabolism with isotopically nonstationary ^{13}C flux analysis. Metab Eng 13:656–665. https://doi.org/10.1016/j.ymben.2011.08.002

Yu Y, You L, Liu D, Hollinshead W, Tang YJ, Zhang F (2013) Development of *Synechocystis* sp. PCC 6803 as a phototrophic cell factory. Mar Drugs 11:2894–2916. https://doi.org/10.3390/md11082894

Zavřel T, Sinetova MA, Búzová D, Literáková P, Červeny J (2015) Characterization of a model cyanobacterium *Synechocystis* sp. PCC 6803 autotrophic growth in a flat-panel photobioreactor. Eng Life Sci 15:122–132. https://doi.org/10.1002/elsc.201300165

Zhang S, Bryant DA (2011) The tricarboxylic acid cycle in cyanobacteria. Science 334:1551–1553. https://doi.org/10.1126/science.1210858